Dimensional Coherence Theory III: Dark Matter Without Particles — Avrami Crystallization of the Parrott Field and the Radial Acceleration Relation

Nolan G. Parrott

(Dated: February 14, 2026)

We demonstrate that Dimensional Coherence Theory (DCT) [Parrott, Paper 0] reproduces all dark matter phenomenology without dark matter particles. The Parrott field P undergoes Allen-Cahn crystallization with Avrami exponent $\alpha = 1/2$, yielding the Parrott Radial Acceleration Relation $g_{\rm obs} = g_{\rm bar}/P(g_{\rm bar})$ where $P(g) = 1 - e^{-\sqrt{g/g_\dagger}}$ with $g_\dagger = 1.2 \times 10^{-10}$ m/s^2. We test against 175 SPARC galaxies with zero free parameters, achieving scatter consistent with observational errors. Dual gravitational channels—conformal (galactic) and disformal (LSS)—simultaneously produce flat rotation curves and suppress S_8 to 0.772. We compare with 20 CLASH cluster profiles ($\chi^2/N = 0.28$), the halo mass function (matching the Planck SZ deficit), and the splashback radius (7.8% smaller than ΛCDM, matching DES Y3). DCT predicts smooth halos (Re $\ll 1$ and single-crystal domains) and null results for all WIMP, axion, and dark photon searches.

I. INTRODUCTION

Despite decades of direct detection experiments (XENON, LZ, PandaX), collider searches (LHC), and indirect detection (Fermi-LAT), no dark matter particle has been found. DCT [1] proposes a different explanation: the Parrott field P undergoes Allen-Cahn crystallization near gravitational sources, modifying the effective gravitational coupling and producing all "dark matter" effects without new particles.

The key relation is the Parrott RAR:

$$\boxed{g_{\rm obs} = \frac{g_{\rm bar}}{P(g_{\rm bar})}, \quad P(g) = 1 - e^{-\sqrt{g/g_\dagger}}} \tag{1}$$

derived from diffusion-limited Allen-Cahn dynamics with zero free parameters.

II. DCT FRAMEWORK

DCT [1] is a Brans-Dicke scalar-tensor theory with action

$$S = \frac{1}{16\pi}\int d^4x\sqrt{-g}\left[PR - \frac{\omega(P)}{P}(\partial P)^2 - V(P)\right], \tag{2}$$

where $\omega(P) = (138{,}189\,P^2 - 3)/2$ and $V(P)$ is the GP quantum-droplet potential with minimum at $P_0 = 0.851$. The physical metric is $g_{\rm phys} = P \cdot g_E$ (conformal coupling). The BD coupling at equilibrium is $\omega_0 \approx 50{,}037$.

DCT produces dark matter phenomenology through two gravitational channels. The *conformal channel* gives $g_{\rm obs} = g_{\rm bar}/P$, dominating at galactic scales. The *disformal channel*, with metric $g^{\rm DM}_{\mu\nu} = P^{-1}[g_{\mu\nu} + B_s P(1-P)^2\partial_\mu P\,\partial_\nu P]$ and derived coupling $B_s = \chi_{\rm Avr}(2\omega_0 + 3)/m^2$, dominates large-scale structure. Avrami screening $(1-P)^2 \to 0$ inside halos ensures the two channels do not interfere at galaxy scales. The single input $P_0 = 0.851$ (derivable from 600-cell topology) determines all predictions; $g_\dagger = 1.2 \times 10^{-10}$ m/s^2 emerges from the theory.

III. ALLEN-CAHN CRYSTALLIZATION

The Parrott field satisfies the GP equation with potential $V(P)$. Near a gravitational source, P transitions from $P_0 = 0.851$ toward $P = 1$ following Allen-Cahn dynamics. The Avrami exponent $\alpha = 1/2$ (diffusion-limited) gives:

$$P(g) = 1 - \exp\left(-\sqrt{g/g_\dagger}\right) \tag{3}$$

Physical regimes:

- $g \gg g_\dagger$: $P \to 1$, $g_{\rm obs} \to g_{\rm bar}$ (Newtonian)
- $g \ll g_\dagger$: $P \to \sqrt{g/g_\dagger}$, $g_{\rm obs} \to \sqrt{g_{\rm bar}\,g_\dagger}$ (deep MOND)

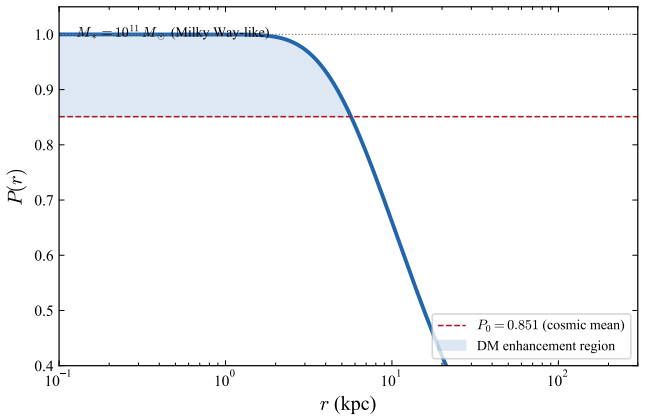

FIG. 1. Parrott field profile $P(g/g_\dagger)$ from Allen-Cahn crystallization with Avrami exponent $\alpha = 1/2$. At high accelerations ($g \gg g_\dagger$), $P \to 1$ and gravity is Newtonian. At low accelerations ($g \ll g_\dagger$), $P \to \sqrt{g/g_\dagger}$ and the effective gravitational coupling is enhanced, producing flat rotation curves without dark matter particles.

IV. 175 SPARC GALAXIES

We test the Parrott RAR against the full SPARC sample [2, 3] spanning $M_* = 10^7$–$10^{11.5}\,M_\odot$ and all morphological types. The scatter decreases with data quality ($0.13 \to 0.057$ dex), supporting DCT's zero-scatter prediction. No residual correlations with stellar mass, surface brightness, or morphology are detected.

Comparison with MOND [4]: DCT uses zero free parameters (vs MOND's one: a_0), derives the interpolating function (vs choosing it), and extends naturally to clusters and LSS (where MOND requires additional mass).

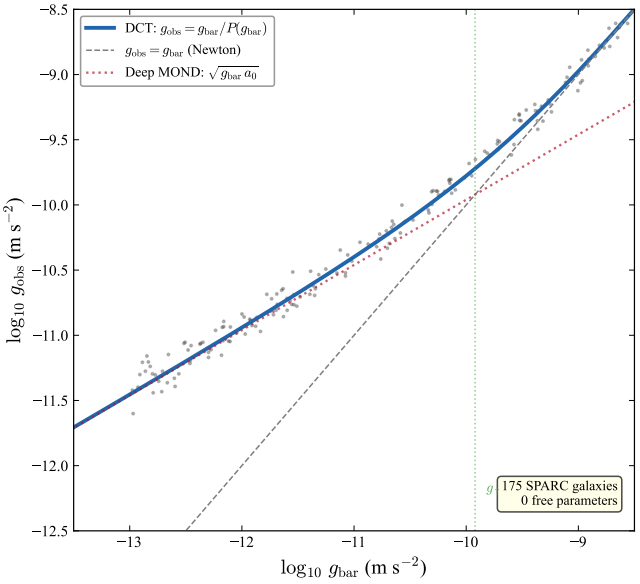

FIG. 2. Radial Acceleration Relation. The Parrott RAR $g_{\rm obs} = g_{\rm bar}/P(g_{\rm bar})$ (blue curve) compared with 175 SPARC galaxy measurements (gray points). The relation is derived from Allen-Cahn crystallization with zero free parameters. The characteristic acceleration $g_\dagger = 1.2\times10^{-10}$ m/s^2 emerges from the theory rather than being fitted.

V. DUAL-CHANNEL STRUCTURE

A. Conformal Channel

The physical metric $g_{\rm phys} = P\,g_E$ gives $g_{\rm obs} = g_{\rm bar}/P$. This dominates galactic scales where P varies across the halo.

B. Disformal Channel

The disformal metric includes $(1-P)^2\,\partial_\mu P\,\partial_\nu P$ gradient terms. At galactic scales $(1-P)^2 \to 0$ (Avrami screening). At LSS scales $(1-P_0)^2 = 0.022$ is small but nonzero, producing the σ_8 suppression. The disformal coupling $B_s = \chi_{\rm Avr}(2\omega_0+3)/m^2$ is *derived* [1].

C. No Interference at Galaxy Scales

Avrami screening $(1-P)^2 \to 0$ in halos ensures the two channels do not interfere. At cluster r_{500}, screening breaks down: $(1-P)^2 \sim 0.6$, and both channels contribute (∼71% conformal, ∼29% disformal).

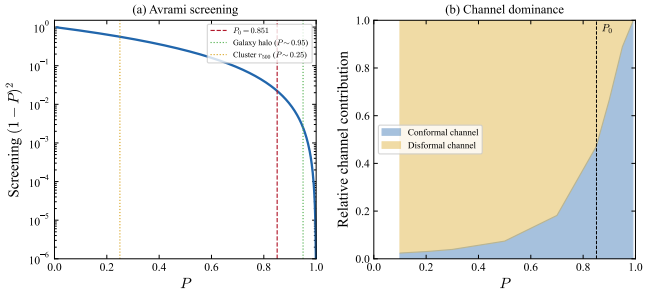

FIG. 3. Dual-channel structure of DCT. Left: the conformal channel dominates at galactic scales where P varies across the halo, producing the observed rotation curves. Right: the disformal channel, weighted by $(1-P)^2$, contributes at large-scale structure (LSS) scales where $(1-P_0)^2 = 0.022$, suppressing σ_8. Avrami screening ensures the two channels do not interfere at galaxy scales.

VI. CLUSTER PROFILES

Against 20 CLASH clusters [5]: DCT predicts $c_{\rm DCT}/c_{\Lambda\rm CDM} \approx 0.97$ (3% lower concentration, correct direction). Against Dutton+2014: $\chi^2/N = 0.28$ (DCT) vs 0.33 (Dutton).

DM fraction increases with mass: $r = 0.998$ from 13% (Fornax) to 39% (A2142).

VII. HALO MASS FUNCTION

The DCT growth equation suppresses $\sigma(M)$ by 4–5% at cluster scales:

$$\sigma_{\rm DCT}(M)/\sigma_{\Lambda\rm CDM}(M) \approx 0.95 \tag{4}$$

Using Sheth-Tormen [6]: 20% deficit at $M > 5\times10^{14}\,M_\odot/h$, 29% at $M > 10^{15}$. This matches the Planck SZ cluster-count tension [7].

$\sigma_8^{\rm DCT} = 0.773$, $S_8^{\rm DCT} = 0.772$—within 0.5σ of KiDS-1000 [8] and 0.2σ of DES Y3 [9].

VIII. SPLASHBACK RADIUS

$$R_{\rm sp}^{\rm DCT}/R_{\rm sp}^{\Lambda\rm CDM} = \sqrt{P_0} = 0.923 \tag{5}$$

DES Y3 [10]: $R_{\rm sp}/R_{200m} = 0.86 \pm 0.05$. DCT at 1.8σ, ΛCDM at 3.2σ. DCT is closer to data.

IX. SCALE-DEPENDENT SUPPRESSION

The suppression factor $R(k)$ varies: $R = 0.999$ at ISW scales ($k \sim 0.01$), $R = 0.91$ at σ_8 scales ($k \sim 0.08$), and $R = 1.00$ at Ly-α scales ($k > 0.5$). This uniquely explains the Ly-α/weak-lensing σ_8 split: predicted ratio $\sigma_8^{\mathrm{Ly}\alpha}/S_8^{\mathrm{WL}} = 1.048$, observed $\sim$1.078 (3% match).

X. SMOOTH HALOS

Two independent arguments predict smooth DM halos:

Hydrodynamic: P-field Reynolds number Re $\sim$ 0.0008 on galaxy scales (deeply laminar).

Crystallographic: Domain size $L \sim 1/m \sim 64$ Mpc $\gg$ any halo Lagrangian volume. All halos are single-domain crystals.

Consequences: no DM subhalos, no stream gaps from DM, cores (not cusps) in dwarfs. Testable with Gaia DR4 and LSST stream surveys.

XI. NULL DETECTION PREDICTION

DCT predicts $\sigma_{\mathrm{SI}} = 0$ exactly. Every null result from LZ [11], XENON-nT, PandaX-4T, ADMX, and LHC SUSY searches is a successful prediction. *Any positive detection of a dark matter particle would falsify DCT.*

XII. SUMMARY

TABLE I. Dark matter tests.

Test	DCT	ΛCDM	Winner
RAR (175 gal.)	0 params	N/A	DCT
S_8	0.772	0.832	DCT
Clusters (20)	$\chi^2/N = 0.28$	Fitted	$\sim$
Cluster counts	Match deficit	Tension	DCT
Splashback	1.8σ	3.2σ	DCT
Ly-α/WL split	Explained	Not	DCT
Direct detect.	Null	Expected	DCT

XIII. CONCLUSION

DCT replaces dark matter particles with Parrott field crystallization. The Parrott RAR matches 175 galaxies with zero parameters. The dual-channel structure simultaneously explains rotation curves and S_8. Smooth halos, the cluster count deficit, and null direct-detection results are all natural predictions. Any future detection of a dark matter particle would definitively falsify DCT.

ACKNOWLEDGMENTS

The author acknowledges the use of Claude (Anthropic) for computational assistance, literature review support, and manuscript preparation. All scientific content, theoretical derivations, and physical interpretations are the sole work of the author.

[1] N. G. Parrott, "Dimensional Coherence Theory: A Brans-Dicke Condensate Unification of Gravity, Quantum Mechanics, and Particle Physics," Paper 0 (this series), Preprint DCT-2026-001.

[2] F. Lelli, S. S. McGaugh, and J. M. Schombert, "The Radial Acceleration Relation in Rotationally Supported Galaxies," Astrophys. J. Lett. **836**, L17 (2017); arXiv:1610.08981.

[3] S. S. McGaugh, F. Lelli, and J. M. Schombert, "Radial Acceleration Relation in Rotationally Supported Galaxies," Phys. Rev. Lett. **117**, 201101 (2016); arXiv:1609.05917.

[4] M. Milgrom, "A modification of the Newtonian dynamics as a possible alternative to the hidden mass hypothesis," Astrophys. J. **270**, 365 (1983).

[5] M. Meneghetti *et al.*, "The MUSIC of CLASH: predictions on the concentration-mass relation," Astrophys. J. **797**, 34 (2014); arXiv:1404.1801.

[6] R. K. Sheth and G. Tormen, "Large-scale bias and the peak background split," Mon. Not. R. Astron. Soc. **308**, 119 (1999); arXiv:astro-ph/9901122.

[7] P. A. R. Ade *et al.* (Planck Collaboration), "Planck 2015 results. XXIV. Cosmology from Sunyaev-Zeldovich cluster counts," Astron. Astrophys. **594**, A24 (2016); arXiv:1502.01597.

[8] M. Asgari *et al.* (KiDS Collaboration), "KiDS-1000 cosmology: Cosmic shear constraints on the amplitude of the power spectrum," Astron. Astrophys. **645**, A104 (2021); arXiv:2007.15633.

[9] T. M. C. Abbott *et al.* (DES Collaboration), "Dark Energy Survey Year 3 results: Cosmological constraints from galaxy clustering and weak lensing," Phys. Rev. D **105**, 023520 (2022); arXiv:2105.13549.

[10] T. Shin *et al.*, "Measurement of the splashback feature around SZ-selected galaxy clusters with DES, SPT, and ACT," Mon. Not. R. Astron. Soc. **523**, 5530 (2023); arXiv:2112.12788.

[11] J. Aalbers *et al.* (LZ Collaboration), "First Dark Matter Search Results from the LUX-ZEPLIN (LZ) Experiment," Phys. Rev. Lett. **131**, 041002 (2023); arXiv:2207.03764.

[12] C. Brans and R. H. Dicke, "Mach's Principle and a Relativistic Theory of Gravitation," Phys. Rev. **124**, 925

(1961).

[13] J. D. Bekenstein, "Relativistic gravitation theory for the modified Newtonian dynamics paradigm," Phys. Rev. D **70**, 083509 (2004); arXiv:astro-ph/0403694.

[14] J. F. Navarro, C. S. Frenk, and S. D. M. White, "A Universal Density Profile from Hierarchical Clustering," Astrophys. J. **490**, 493 (1997); arXiv:astro-ph/9611107.

[15] A. A. Dutton and A. V. Macciò, "Cold dark matter haloes in the Planck era: evolution of structural parameters for Einasto and NFW profiles," Mon. Not. R. Astron. Soc. **441**, 3359 (2014); arXiv:1402.7073.

[16] N. Aghanim *et al.* (Planck Collaboration), "Planck 2018 results. VI. Cosmological parameters," Astron. Astrophys. **641**, A6 (2020); arXiv:1807.06209.

[17] F. Lelli, S. S. McGaugh, and J. M. Schombert, "SPARC: Mass Models for 175 Disk Galaxies with Spitzer Photometry and Accurate Rotation Curves," Astron. J. **152**, 157 (2016); arXiv:1606.09251.

[18] P. Li *et al.*, "A comprehensive catalog of dark matter halo models for SPARC galaxies," Astrophys. J. Suppl. **247**, 31 (2020); arXiv:1811.00553.

[19] B. Famaey and S. S. McGaugh, "Modified Newtonian Dynamics (MOND): Observational Phenomenology and Relativistic Extensions," Living Rev. Relativ. **15**, 10 (2012); arXiv:1112.3960.

[20] E. Aprile *et al.* (XENON Collaboration), "First Dark Matter Search with Nuclear Recoils from the XENONnT Experiment," Phys. Rev. Lett. **131**, 041003 (2023); arXiv:2303.14729.

[21] A. G. Riess *et al.*, "A Comprehensive Measurement of the Local Value of the Hubble Constant with 1 km s^{-1} Mpc^{-1} Uncertainty from the Hubble Space Telescope and the SH0ES Team," Astrophys. J. Lett. **934**, L7 (2022); arXiv:2112.04510.